Indonesian Journal of Electrical Engineering and Informatics (IJEEI)
Vol. 12, No. 2, June 2024, pp. 409~424
ISSN: 2089-3272, DOI: 10.52549/ijeei.v12i2.5465

Optimal Power Flow with Integrated Large Scale PV Systems: Case of the Algerian Solar Field

Aicha Mallem[1], Omar Boudebbouz[2]
[1,2]Department of Electrical Engineering, Faculty of Technology, LES Laboratory,
University of 20 Aout 1955 Skikda, Algeria

Article Info

Article history:

Received Feb 25, 2024
Revised Apr 23, 2024
Accepted May 10, 2024

Keywords:

Optimal power flow
Emission
Quadratic cost function
Cubic cost function
Particle swarm optimization
Algerian solar energy potential

ABSTRACT

The integration of large-scale solar-photovoltaic generation in the traditional power system complicates the optimal power flow (OPF) problem formulation. In the present paper, the OPF based on the quadratic and cubic fuel cost functions integrating solar energy potential of the south of Algeria is presented. Solar energy has a stochastic behavior described in the proposed methodology by the Beta probability distribution function (βPDF). The corresponding objective functions consider the penalty and reserve costs of large-scale solar-photovoltaic generations. The proposed OPF is solved by particle swarm optimization (PSO) algorithm. Computer simulations have been performed on an Algerian 59 bus test system considering some candidates solar energy source emplacements. The comparison between OPF solutions based on the two aforementioned cost functions has been established. The cubic fuel cost function case shows more environmental pollution reduction as well as satisfying interconnected power demands. Thanks to the PSO algorithm properties used for the OPF resolution, the Algerian solar field seems to be a good opportunity for large-scale solar-photovoltaic generation installations in an oligopolistic and eco-friendly sense.

Corresponding Author:

Aicha Mallem,
Department of Electrical Engineering,
Faculty of Technology, LES Laboratory, University of 20 Aout 1955 Skikda,
BP 26. El Hadaiek Road- 21000, Skikda, Algeria.
Email: a.mallem@univ-skikda.dz

1. INTRODUCTION

The electric energy is a key aspect of economic and sustainable development worldwide. The growth of population and economic activities further increases its use. Securing sustainable energy sources is an important priority in power system operation.

The optimal power flow (OPF) is among the main monitoring and evaluation tools in power schedulers and energy management systems [1]. It provides precious information for power system control and economic energy management. Mathematically, OPF is a very large non-linear optimization problem subject to equality and inequality constraints. Several methods of optimization have been applied to resolve the problem such as, Linear Programming [2], Quadratic Programming [3], Genetic Algorithm [4], Tabu Search [5], Particle Swarm Optimization [6, 7], Simulated Annealing [8], Artificial Bee Colony [9] and Ant Colony Search [10], etc. However, the integration of solar energy mega-structures to the traditional power system complicates the optimal power flow (OPF) problem formulation due, particularly their stochastic nature.

The choice of the regions with the highest potential for installing the renewable power plants is a fundamental topic. It requires using a sound approach in order to guarantee the efficiency of these projects.

Algeria is the largest country in North Africa and the Mediterranean region, with an area of 2381,741 km^2, where the desert occupies approximately 86% of the total area. It receives 2500 KWh/m^2 of annual sunshine. The average annual amount of solar energy received globally on a horizontal surface is about 2650 kWh/m^2 per year [11]. It is reported that Algeria has a large radiation potential, which is estimated at 5000

times the country's electrical power consumption and 60 times Europe's electricity consumption [12]. With this huge solar potential, Algeria could address the local increasing energy needs, preserve the fossil fuel sources for other uses, and avoid carbon dioxide (CO_2) emissions. In addition, it can become one of the major countries in the world market for renewable energy by the export of this source, and consequently, an ideal location for solar mega-structures installation. According to this view, the main objectives of the present work will concern:

- The description of the energy sector status and solar field of Algeria.
- Proposing variants of solar mega-structures integration in an actual Algerian power system.
- Formulation of the OPF problem, including the random variable of solar power.
- Implementation of the particle swarm optimization (PSO) algorithm for resolving the OPF issue on an Algerian electrical network of 59 buses for optimization purposes.

2. DESCRIPTION OF ENERGY SECTOR STATUS AND SOLAR FIELD OF ALGERIA

2.1. Energy mix and Oligopolistic aspect

The Algerian energy mix mainly comprises gas, oil, and electricity [13]. The latter comes primarily from fossil fuels. Table 1 presents the corresponding electricity generation in 2021. This makes Algeria one of the important CO_2 emitters in the world, with 139.67 million tons of CO_2 as reported in 2021 [14]. The current national power production capacity is 25 GW, while the power consumption peak reached 18 GW during the summer of 2023 [15]. This power margin guarantees social and economic development and can be exported to neighboring countries in Africa and Southern Europe [16].

Table.1 Algeria's Electricity generation in 2021 [17].

Type of primary energy	Electricity generation	
	(GWh)	(%)
Fuel fossil	84729	99
Hydro and marine	9	0
Bioenergy	0	0
Geothermal	0	0
Wind	11	0
Solar	760	1
Total	85509	100

Algeria is experiencing an important augmentation in electricity consumption, predicted to multiply by two by 2030 due to demographic growth and economic development, as shown in Figure 1.

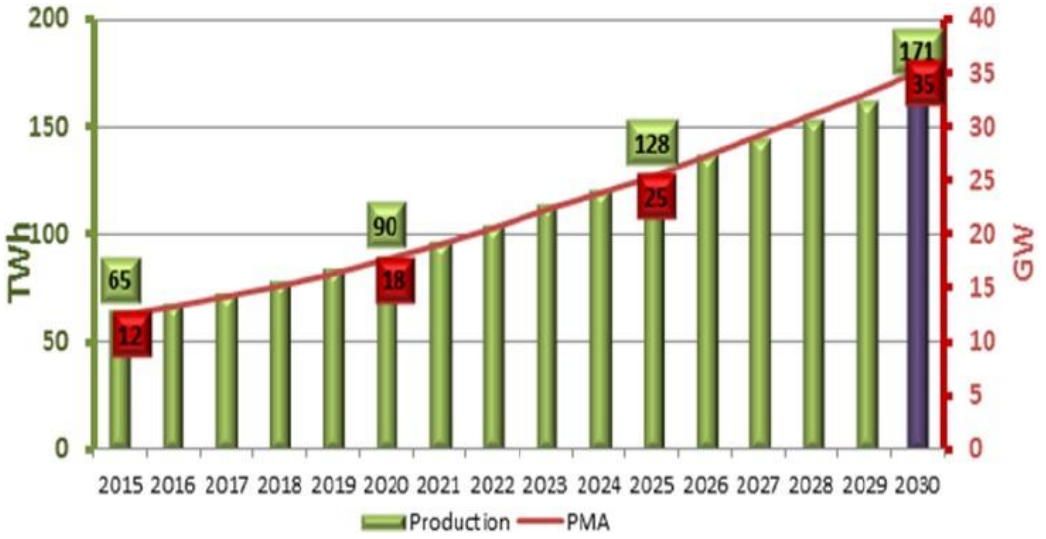

Figure 1. Evolution of electricity consumption in Algeria 2015-2030 [18].

Algeria's electricity network is managed by the state-owned National Electricity and Gas Company (SONELGAZ). At the end of 2022, it was indicated that Algeria could to export its surplus electricity generation to Europe [19] through a marine electric line until the Italian coast. It also indicated to the establishment of a high voltage line (approximately 1300 km) connecting the cities of the south to those of the North and subsequently connecting Algeria to African countries located in the south of Algeria [20].

2.2. Solar energy potential of Algeria and geographical aspect

Algeria has a strategic location in the center of North Africa and facing Europe. The southern states occupy almost more than 50 % of the total area. It is characterized by abundant sunshine with an annual duration exceeds 2000 h and reaches 3900 h (sunshine duration of more than 14 h/day in the summer, and more than 10 h/day in the winter) [11]. The global horizontal solar irradiance per day is also abundant throughout the year, as shown in Figure 2.

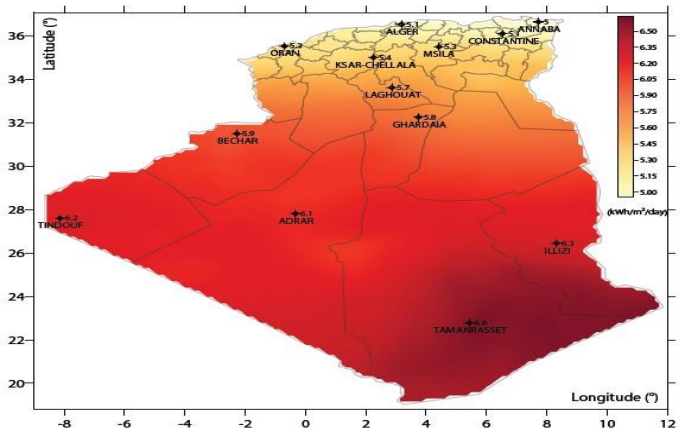

Figure 2. Solar energy potential in Algeria (KWh/m^2) [21].

Algeria's location, combined with its nearness to Europe's southern countries, enables the production of large quantities of electricity from solar energy. The southern states also called the Sahara, could be a major source of clean energy in the future.

3. EXPLOITATION OF SAHARA SOLAR POTENTIAL

The Algerian electrical network consists of three essential networks: Northern Interconnected Network (RIN), Pole In Salah/ Adrar /Timimoun (PIAT), and southern isolated networks (RIS) [22]. The Algerian network is sparse in the Sahara, as shown in Figure 3. The Algerian energy flow is predominantly from North to South. But this matter must be reviewed, especially with the great solar potential in the Sahara region.

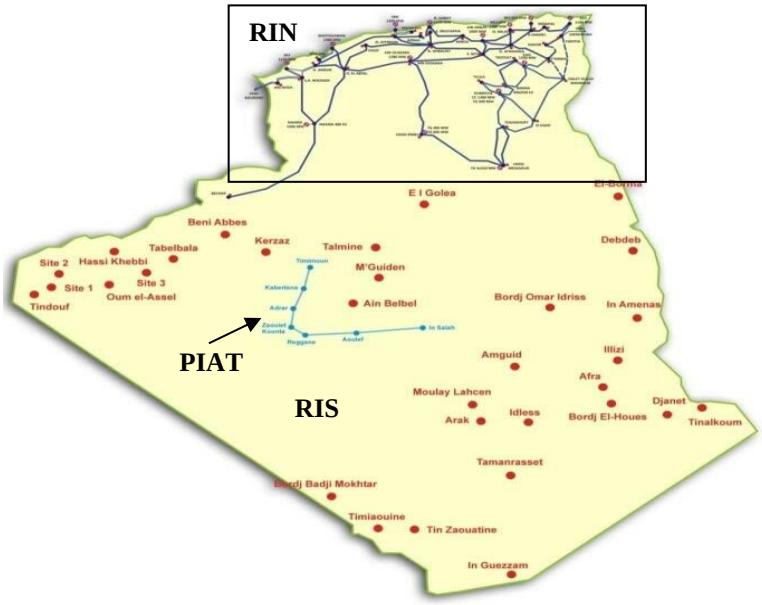

Figure 3. Algeria's electrical network [21].

A reorientation of the electrical flows with an installation of large solar mega-structures in the Sahara is urgent. Figure 4 shows two proposed variants based on considering some factors to choose the appropriate location for establishing solar mega-structures, such as future global radiation, ambient temperature, natural hazards, and land suitability regarding terrain and slope. Each mega-structure consists of hundreds of millions

of solar panels designed like a black box as a generator node. The corresponding output Power must be maximized by means of the well-known Maximum Power Point Tracking (MPTT) programs for the each considered operating point in the simulation process. High-voltage direct current (HVDC) connections are also used to transmit electricity over long distances from each solar mega-structure in the Sahara to the northern consumption centers to reduce transmission losses. Table 2 presents the geographical coordinates and the limits of monthly temperature values of six locations of solar mega-structures.

Table 2. Data of the studied plants [23, 24].

City	Latitude (deg.)	Longitude (deg.)	Altitude (m)	Min. temperature (C°) (December)	(July)	Max. temperature (C°) (December)	(July)
Ouargla	31.93	5.40	144	5.90	28.10	19.80	44.00
Adrar	27.82	-0.18	279	7.30	29.60	22.10	46.40
Tindouf	27.70	-8.17	443	8.60	27.10	21.50	44.20
Illizi	26.50	8.42	558	6.90	26.70	21.90	41.60
Tamanrasset	22.80	5.43	1362	7.40	23.20	21.90	35.50
Ghardaia	32.40	3.80	468	7.30	28.40	17.60	41.50

3.1. First variant

The first proposed variant is the integration of three solar PV mega-structures in three cities from the eastern to western of the Sahara region. The three cities are Illizi, Tamanrasset, and Tindouf, as shown in Figure 4 (a). In Algeria, the minimum solar radiation is reached at sunrise in Illizi in the east of the country, at around 05:30 in the summer and 06:30 in the winter, and at sunset in Tindouf in the west of the country, at around 20:30 in the summer and 19:30 in the winter. As these two cities are 1800 km apart, it is possible to benefit from a long duration of radiation, which can reach 16 hours during the day. The coordinating of the production of electricity from sunrise in Illizi until sunset in Tindouf, is considered a perfect opportunity to generate solar PV energy on the largest scale. In addition, these two cities enjoy a moderate summer climate due to the influence of offshore winds from the western Atlantic Ocean, which provides ideal conditions for performing photovoltaic (PV) panels without stress.

3.2. Second variant

The second proposed variant is the integration of three solar thermal mega-structures in three cities of the middle region of Sahara. The three cities are Ouargla, Ghardaïa, and Adrar, as shown in Figure 4 (b). The temperature in these cities can reach 65 C°, contributing to the optimal solar panel performance conditions.

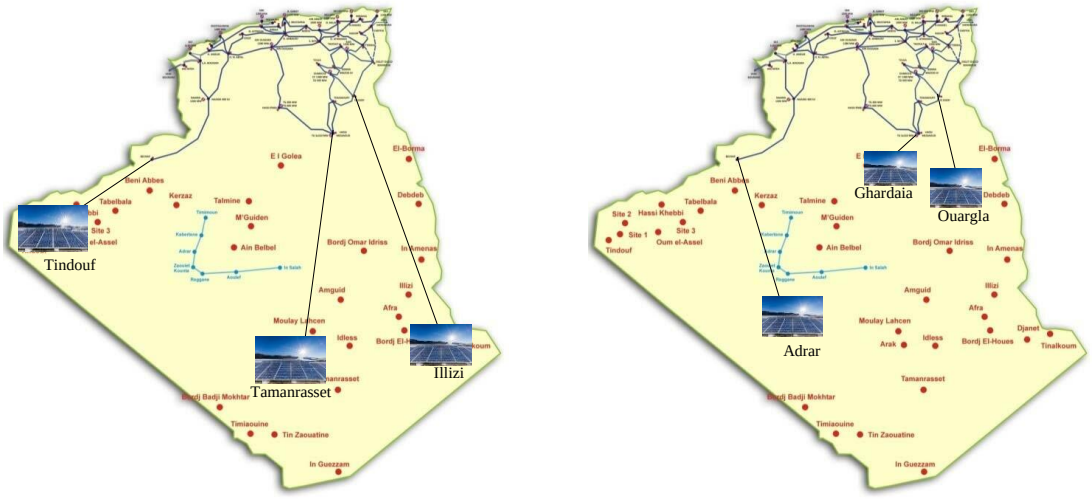

(a) (b)

Figure 4. Integration of mega-structures in Sahara.

3.3. Operational scenario

The operational of scenario the two variants during day and night, which combines the advantages of solar and conventional energy to meet electricity needs, is as follows:

- Generation of electricity from solar mega-structures using solar panels during the day.
- Using conventional energy sources in the north, to provide electricity at night.
- Using control systems to ensure an efficient and balanced distribution.

- Regular maintenance and continuous power system monitoring to ensure the optimum performance.

The Algerian network has no restrictions on the situation during the night period since its absolute peak does not exceed 18 GW out of 25 GW installed. Algeria is considered a large producer of electricity. In addition, the minimal amount of electrical energy consumed is at most 12 to 13 GW out of 25 GW installed. The minimum is always produced at night when electricity consumption is very weak or approaches zero in the Sahara region due to its significant decrease in population density.

3.4. Benefits of proposed variants

The main benefits for Algeria from the two proposed variants are:

- Reducing the dependence on fossil fuels to generate electricity by harnessing the natural solar potential to ensure electricity supply.
- Reducing CO_2 emissions by displacing fossil fuel-based electricity generation.
- Achieving industrial, agricultural, and economic development in the Sahara by expanding electrical energy access to isolated desert areas.
- Guarantee the power system security, especially regarding the production of electricity during the night.
- Exporting electricity, liberating the country's economy from dependence on fossil fuels, and sweeping the European and African markets to raise the country's status and become a significant energy pole.

4. OPTIMAL POWER FLOW FORMULATION

The purpose of OPF can be summarized as the minimization of particular objective fonctions while meeting the equality and inequality constraints [25]. It may be written as:

$$\text{Minimize of } F(x) \quad (1)$$

$$\text{Subject to: } E_i(x) = 0, \quad i = 0, \ldots, n \quad (2)$$

$$EI_j(x)_{Lower} \leq EI_j(x) \leq EI_j(x)_{Higher}, \quad j = 0, \ldots, m \quad (3)$$

Where $F(x)$ is the objective function. $E_i(x)$ and $IE_j(x)$ are the equality and inequality constraints, respectively. $EI_j(x)_{Higher}$ and $EI_j(x)_{Lower}$ are the higher and lower inequality constraints, respectively. n and m are the number of equality and inequality constraints, respectively.

4.1. Objective functions

4.1.1. Objective function 1: Generation cost

This function is expressed as reducing of the thermal and solar generation cost function while considering into account the factors implicated in the under and over estimation of solar powers. It can be formulated as:

$$C_{tot} = C_{Th\,tot} + \sum_{i=1}^{N_S} C_{RSi} + \sum_{i=1}^{N_S} C_{PSi} \quad (4)$$

The first term in Equation (4) is the cost function of thermal units. Generally, the OPF problem is presented with a quadratic cost function, which can be given as:

$$C_{Th\,tot} = \sum_{i=1}^{N_{Th\,G}} (\alpha_i + \beta_i P_{Th\,Gi} + \gamma_i P_{Th\,Gi}^2) \quad (5)$$

Where α_i, β_i and γ_i are the cost coefficients of thermal unit i. $N_{Th\,G}$ and $P_{Th\,Gi}$ are the number of thermal units and the active power of i^{th} thermal unit, respectively.

The OPF solution can be ameliorated by the use of higher-order generation cost functions. The cubic cost function can display with more accurately the actual thermal unit response, and it can be given by:

$$C_{Th\,tot} = \sum_{i=1}^{N_{Th\,G}} (\alpha_i + \beta_i P_{Th\,Gi} + \gamma_i P_{Th\,Gi}^2 + \delta_i P_{Th\,Gi}^3) \quad (6)$$

Where α_i, β_i, γ_i, and δ_i are the cost coefficients of i^{th} thermal unit.

The second term in Equation (4) is the total reserve cost function. It indicates the cost resulting from the overestimation of solar power [26, 27]. The reserve cost of i^{th} solar plant (C_{RSi}) can be calculated by:

$$C_{RSi} = h_{RSi}.(P_{SHi} - P_{Savi}) = h_{RSi}.\int_0^{P_{SHi}} (f_S(P_S).(P_{SHi} - P_S))dP_S \quad (7)$$

Where h_{RSi} is the reserve cost of i^{th} solar plant, $P_{Sav\ i}$ and P_{SHi} are the available and the scheduled power from the i^{th} solar plant, respectively. $f_s(P_S)$ is the probability distribution function (PDF) of solar power, P_S is the expected output power from the solar plant, which is a random value that belongs to the interval [0, P_{SHi}].

The third term in Equation (4) is the total penalty cost function. It signifies the cost resulting from the underestimation of solar power [26, 27]. The penalty cost of i^{th} solar plant (C_{PSi}) can be calculated as:

$$C_{PSi} = h_{PSi}(P_{Savi} - P_{SHi}) = h_{PSi}.\int_{P_{SHi}}^{P_{SRi}}(f_S(P_S).(P_S - P_{SHi}))dP_S \quad (8)$$

Where h_{PSi} is the penalty cost coefficient of i^{th} solar plant, P_{SRi} is the rated output power from the i^{th} solar plant. P_S is the expected output power from the solar plant, which is a random value that belongs to the interval [P_{SHi}, P_{SRi}]. The output power from the solar generator affects the solar irradiance (s_r), and it can be determined as [28]:

$$P_S = \begin{cases} P_{Sn}\frac{{s_r}^2}{s_{s\,tan}\cdot s_c}, & 0 < s_r < s_c \\ P_{Sn}\frac{s_r}{s_{s\,tan}}, & s_r \geq s_c \end{cases} \quad (9)$$

Where P_{Sn} is the nominal solar power, s_c is a certain irradiance point, and $s_{s\,tan}$ is the solar irradiance in a standard environment. The probability of solar irradiance (s_r) can be modeled by Beta probability distribution function (βPDF), and it is expressed as [29]:

$$f_{BT}(s_r) = \frac{\Gamma(a_{BT}+b_{BT})}{\Gamma(b_{BT})\Gamma(a_{BT})}.(1-s_r)^{(b_{BT}-1)}.{s_r}^{(a_{BT}+1)} \quad (10)$$

Where Γ is the Gamma function. s_r is the solar irradiance in KW/m ^{2}, which is a random variable belonging to the interval [0, 1]. a_{BT} and b_{BT} are two parameters of βPDF, which can be given by:

$$\begin{cases} a_{BT} = \frac{\tau.b_{BT}}{1-\tau}, a_{BT} \geq 0 \\ b_{BT} = (1-\tau)\left(\frac{\tau(1+\tau)}{\theta^2}\right), b_{BT} \geq 0 \end{cases} \quad (11)$$

Where τ and θ are mean and standard deviation of solar irradiance, respectively.

4.1.2. Objective function 2: Generation cost with emission

This function is expressed as the minimization of the fuel cost of generation and the release of a few quantities of polluting gases in the atmosphere. It is achieved by combining the total cost function and emission function with the help of the price penalty factor (h_p). The emission function can be expressed by:

$$E_{tot} = \sum_{i=1}^{N_{Th\,G}} 10^{-2}.(a_i + b_i P_{Th\,Gi} + c_i P_{Th\,Gi}^2 + d_i\, exp(\, e_i P_{Th\,Gi})) \quad (12)$$

Where a_i, b_i, c_i, d_i, and e_i are the emission coefficients of i^{th} thermal unit.

The total objective function without considering solar power can be formulated as:

$$C_{tot} = w_f.(C_{Th\,tot}) + (1-w_f).h_p.(E_{tot}) \quad (13)$$

The total objective function with considering solar power can be formulated as:

$$C_{tot} = w_f.\left(C_{Thtot} + \sum_{i=1}^{N_S}(C_{RSi} + C_{PSi})\right) + (1-w_f).h_p.(E_{tot}) \quad (14)$$

Where h_p and w_f are the price penalty factor and the weight factor which belongs to the interval [0,1]. This price penalty factor is defined as:

$$h_p = \frac{C_{Th\,tot}(P_{Th\,Gi}^{max})}{E_{tot}(P_{Th\,Gi}^{max})} \quad (15)$$

4.2. Equality constraints

The equality constraints present the active and reactive power balance as follows:

$$\sum_{i=1}^{N_{Th\,G}} P_{Th\,Gi} = P_{Loss} + P_{Load} \quad (16)$$

$$\sum_{i=1}^{N_{Th\,G}} Q_{Th\,Gi} = Q_{Loss} + Q_{Load} \quad (17)$$

Where P_{Load} and Q_{Load} are the active and reactive load power, respectively. P_{Loss} and Q_{Loss} are the active and reactive transmission line losses, respectively.

4.3. Thermal generator Inequality constraints

The active power and voltage magnitude of thermal generators are limited by their upper and lower limits.

$$P_{Th\,Gi}^{min} \leq P_{Th\,Gi} \leq P_{Th\,Gi}^{max} \text{ , i=1}.....N_{Th\,G} \quad (18)$$

$$V_{Th\,Gi}^{min} \leq V_{Th\,Gi} \leq V_{Th\,Gi}^{max} \text{ i=1}.....N_{Th\,G} \quad (19)$$

4.4. Solar power Inequality constraints

The solar output power varies from zero to the maximum value of the installed capacity of solar plants.

$$0 \leq P_{Si} \leq P_{Si}^{max} \quad (20)$$

5. PARTICLE SWARM OPTIMIZATION (PSO)

Particle swarm optimization (PSO) is an optimization approach proposed by Kennedy and Eberhart [30]. It is inspired by social conduct and a procedure followed by some animals organized colonies, like birds or fish, when searching for food. PSO is a search method based on inhabitants. The process starts with an initial population, then searching for the optimal by updating generations. The population is named a swarm of potential solutions. These last solutions are called particles, which are placed randomly in the search space and modified after each iteration of the algorithm. They fly and change their positions. Each particle confirms its position by its particular participation and the participation of neighboring particles. It evolves according to its best neighbor, its best position, and its previous position. At any time, each particle knows its best position P^b, and global best position G^b, among all the particles of the swarm. During iterations, the particles change their positions according to the new velocities.

The position vector(x_{pr}) and velocity vector (v_{pr}) of particle (pr) in a search space of dimension (S_p) are given by:

$$x_{p_r} = (x_{p_r1}, x_{p_r2}.... x_{p_rS_p}) \quad (21)$$

$$v_{p_r} = (v_{p_r1}, v_{p_r2}.... v_{p_rS_p}) \quad (22)$$

At each iteration, a comparison is required between the value given by the current particle and the previous value.

The velocity and position of the particle p_r at (t+1) iteration are written as follows:

$$v_{p_r}^{(t+1)} = \omega . v_{p_r}^{(t)} + c_1 . d_1 . (P^b{}_{p_r}^{(t)} - x_{p_r}^{(t)}) + c_2 . d_2 . (G^b{}_{p_r}^{(t)} - x_{p_r}^{(t)}), p_r = 1.... N_{pr} \quad (23)$$

$$x_{p_r}^{(t+1)} = x_{p_r}^{(t)} + v_{p_r}^{(t+1)} \quad (24)$$

Where $v_{pr}^{(t)}$ and $x_{pr}^{(t)}$ are the velocity of the particle i at iteration t and the current position of particle i at iteration t, respectively. t and N_{pr} are the number of iterations and number of particles, respectively. d_1 and d_2 are two random values with [0,1] range. c_1 and c_2 are two acceleration constants, which are typically adjusted to 2 based on previous experiences [31]. ω is the inertia weight factor used to regulate velocity, which can be determined as:

$$\omega = \omega^{Max} - t . (\frac{\omega^{Max} - \omega^{Min}}{t^{Max}}) \quad (25)$$

Where t and t^{Max} are the numbers of current and maximum iteration, respectively. ω^{Max} and ω^{Min} are maximum and minimum inertia weight factors, respectively.

The process of the PSO algorithm is repeated until a maximum iteration is completed and the stopping criteria are satisfied. The PSO algorithm is represented in Figure 5.

Initialization
Choose PSO parameters: N_{pr}, t^{Max}, c_1, c_2, ω^{Min} and ω^{Max}
Generate randomly an initial population of particles.
Set the initial values of each particle's position x_{pr} and velocity v_{pr}
Initialize local best position P^b and find global best position G^b.
Iteration $t = 0$
while $t < t^{Max}$
Calculate the inertia ω
for each particle *pr*
Calculate the new velocity and new position.
Evaluate the objective functions at new positions.
Check /update $P^{b(t)}$ and $G^{b(t)}$
end for
update t=t+1
end while

Figure 5. PSO algorithm.

6. SIMULATION RESULTS

In order to identify the impact of the installation of large-scale PV systems on the Algerian power system OPF, the variant illustrated in Figure 4 (a) is considered. The Algerian 59 bus electrical network with 10 generators and 83 branches [32], has been selected. A customized program has been established in the MATLAB software. The voltage magnitude limits for generator nodes are between 0.95 p.u and 1.1 p.u. The voltage magnitude limits for load nodes are between 0.9 p.u and 1.1 p.u. The total active load is equal 684.1 MW. The active power generation limits, the quadratic and cubic cost coefficients, and the emission coefficients of generators are taken from [33] and presented in Table 3 and Table 4, respectively. Figure 6 shows the modified 59 bus electrical system which includes three PV mega-structures of 130 MW each installed at buses 19, 36, and 51, respectively.

Table 3. Cost coefficients and power generation limits.

Node number	$P_{Th\,G}^{min}$ (MW)	$P_{Th\,G}^{max}$ (MW)	α ($/h)	β ($/MW.h)	γ ($/MW^2.h)	δ ($/MW^3.h)
1	8	72	0	1.5	0.0085	0.00000085
2	10	70	0	2.5	0.0170	0.00000150
3	30	510	0	1.5	0.0085	0.00000085
4	20	400	0	1.5	0.0085	0.00000085
13	15	150	0	2.5	0.0170	0.00000150
27	10	100	0	2.5	0.0170	0.00000150
37	10	100	0	2.0	0.0030	0.00000026
41	15	140	0	2.0	0.0030	0.00000026
42	18	175	0	2.0	0.0030	0.00000026
53	30	450	0	1.5	0.0085	0.00000085

Table 4. Emission coefficients.

Node number	*a*	*b x10*$^{-2}$	*c x10*$^{-4}$	*d*	*e x10*$^{-2}$
1	4.091	–5.554	6.490	2.10^{-4}	2.857
2	2.543	–6.047	5.638	5.10^{-4}	3.333
3	4.258	–5.094	4.586	1.10^{-6}	8.000
4	5.326	–3.550	3.380	2.10^{-3}	2.000
13	4.258	–5.094	4.586	1.10^{-6}	8.000
27	6.131	–5.555	5.151	1.10^{-5}	6.667
37	4.091	–5.554	6.490	2.10^{-4}	2.857
41	2.543	–6.047	5.638	5.10^{-4}	3.333
42	4.258	–5.094	4.586	1.10^{-6}	8.000
53	5.326	–3.550	3.380	2.10^{-3}	2.000

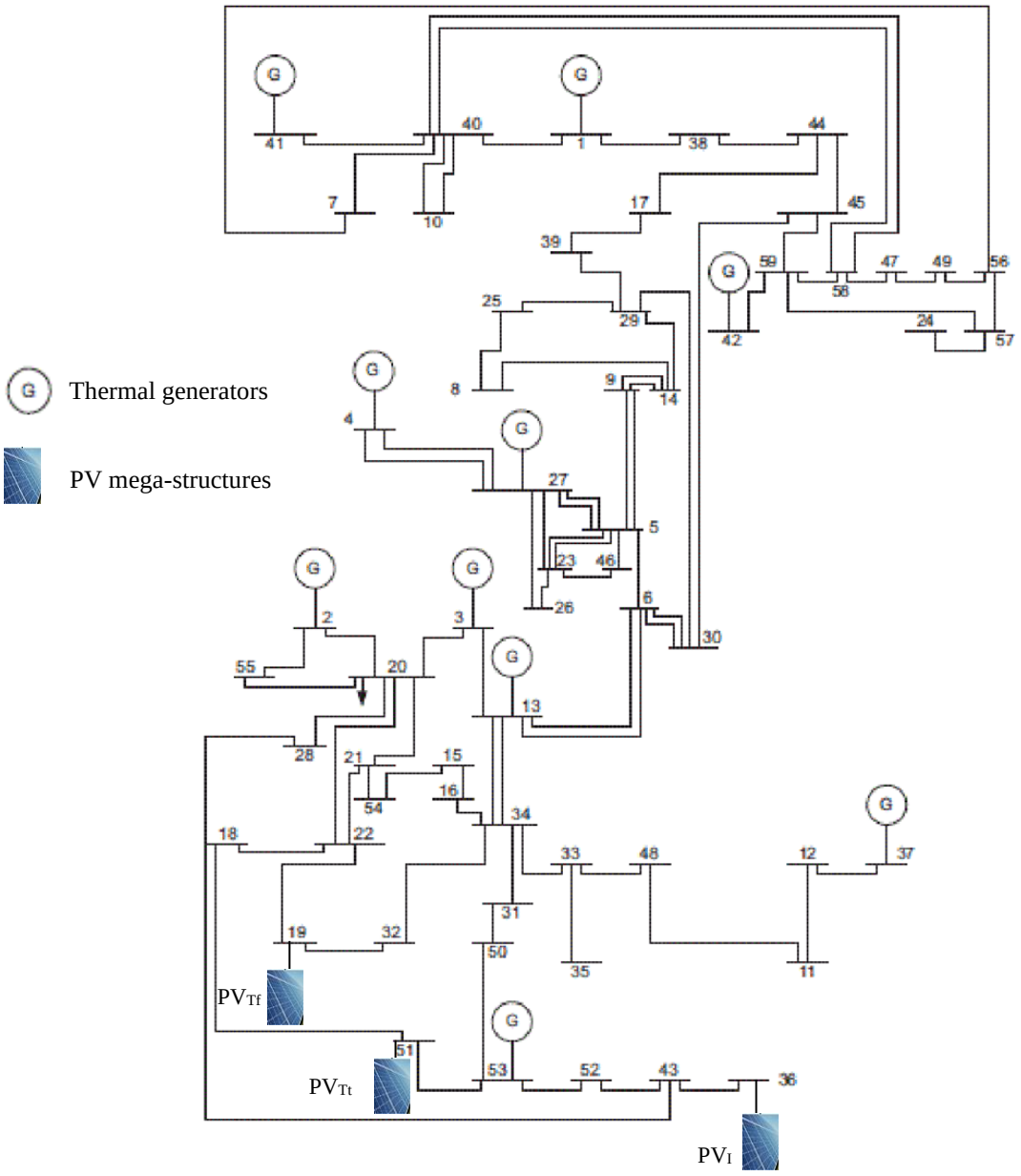

Figure 6. Modified Algerian 59 bus power system with three PV mega-structures.

Table 5 presents the average hourly mean and standard deviation of the three PV mega-structures. Each solar PV mega-structure has penalty and reserve cost coefficients of 1.5 and 4, respectively.

Table 5. Average hourly mean and standard deviation from PV mega-structures.

City	PV mega-structure	Mean	Standard deviation
Tindouf	PV_{Tf}	0.698	0.059
Illizi	PV_{I}	0.680	0.063
Tamanrasset	PV_{Tt}	0.689	0.061

Five cases are evaluated for the OPF problem using PSO algorithm. The control variables considered are generators' active power and voltage magnitude. The PSO parameters considered in this simulation are:

- Acceleration constants $c_1 = c_2 = 2$
- Minimum and maximum values of inertia weight are: $\omega^{Min} = 0.4$ and $\omega^{Max} = 0.9$
- Particle numbers: 100
- Iteration numbers: 200

6.1. Minimization of generation cost without considering solar PV mega-structures

The OPF problem is solved by considering only 10 thermal generators. The aim is to reduce the thermal generation cost with quadratic and cubic cost functions. Table 6 shows the simulation results.

a. Case 1.1: Minimization with a quadratic cost function

The objective function to be reduced is given by Equation (5). Figure 7 (a) illustrates the convergence of the thermal cost function. From Table 6, the thermal generation cost and total active power loss are 1786.7 $/h and 19.4648 MW, respectively. The bus voltage magnitudes are illustrated in Figure 10 where the minimum value is 0.9633 p.u at bus 13.

b. Case 1.2: Minimization with a cubic cost function

The objective function to be reduced is given by Equation (6). Figure 7 (b) illustrates the convergence of the thermal cost function. Table 6 shows that the results of OPF with a cubic cost function are better than those obtained with a quadratic cost function. The thermal generation cost and total active power loss are 1738.7 $/h and 18.5143, respectively. The bus voltage magnitudes are illustrated in Figure 10, where the minimum value is 0.9258 p.u at bus 14.

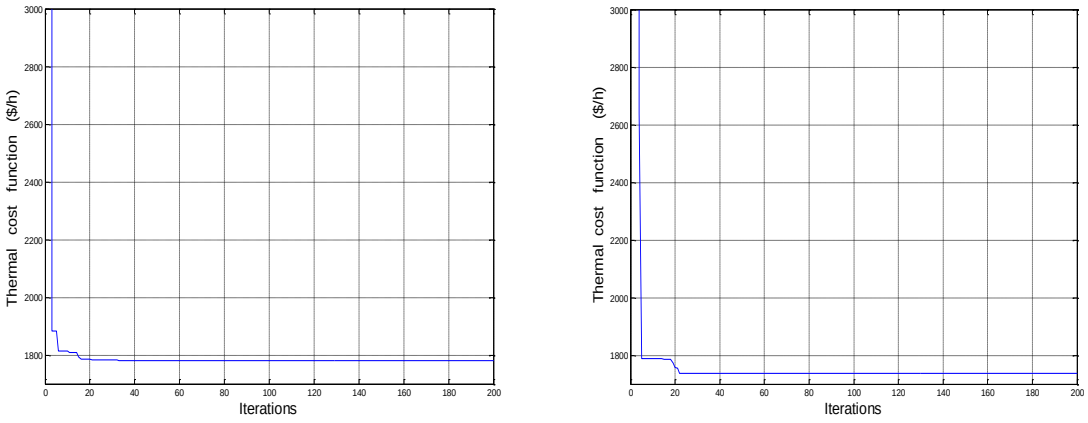

(a) (b)

Figure 7. Convergence of thermal cost function without integration of solar PV mega-structures.

6.2. Minimization of generation cost with considering two solar PV mega-structures

The OPF problem in this case is resolved **by** taking into account 10 thermal generators and two solar PV mega-structures. The aim is to reduce the total generation cost with quadratic and cubic cost functions. The expenses associated with under and overestimating solar PV powers are included in the total generation c ost, along with the cost of thermal generators. The PV mega-structures are connected to the test power system at buses 19 and 36 in Tindouf and Illizi cities, respectively. Table 6 shows the simulation results.

a. Case 2.1: Minimization with a quadratic cost function

The objective function is given by Equation (4) with a quadratic cost function. Figure 8 (a) shows the total cost function convergence. Table 6 shows that integrating two solar PV mega-structures reduces the total active power loss and cost. The total active power loss has lowered from 19.4648 MW in Case 1.1 to 9.4010 MW. The thermal generation cost is 1141.2 $/h, which is considered 36.128 % lower than the thermal generation cost in Case 1.1. The solar PV cost is 312.8543 $/h. The bus voltage magnitudes are illustrated in Figure 10 where the minimum value is 0.9129 p.u at bus 38.

b. Case 2.2: Minimization with a cubic cost function

The objective function is given by Equation (4) with a cubic cost function. Figure 8 (b) shows the total cost function convergence. From Table 6, the total power loss and generation cost are less with integrating two solar PV mega-structures with a cubic cost function. The total active power loss has lowered from 18.5143 MW in Case 1.2 to 9.2150 MW. The thermal generation cost is 1138.2 $/h, which are considered 34.537 % lower than the obtained thermal generation cost in Case 1.2. The bus voltage magnitudes are illustrated in Figure 10 where the minimum value is 0.9149 p.u at bus 38.

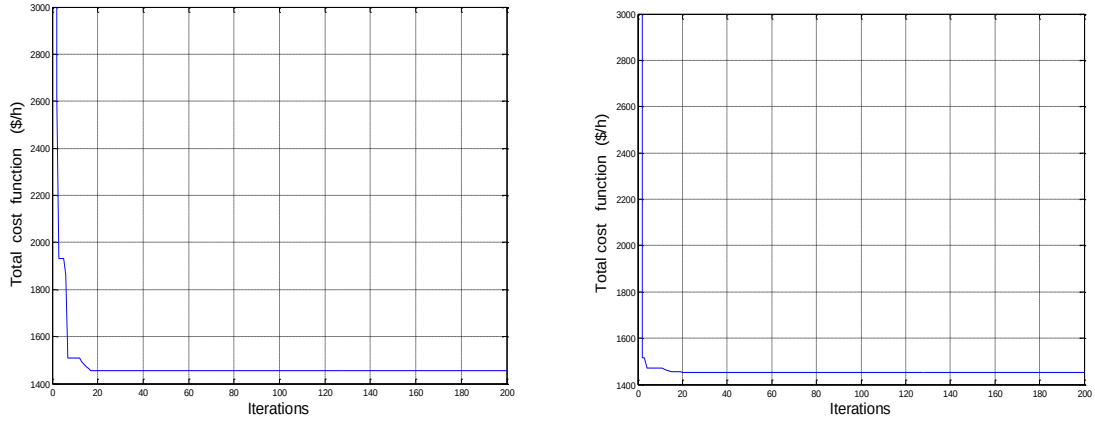

(a) (b)

Figure 8. Convergence of total cost function with integration of two solar PV mega-structures.

6.3. Minimization of generation cost with integration of three PV mega-structures

In this case, the OPF is resolved by accounting for 10 thermal generators and three solar PV mega-structures. These mega-structures are connected to 59 bus power system at buses 19, 36 and 51 in Tindouf, Illizi and Tamanrasset cities, respectively. Table 6 tabulates the results.

a. Case 3.1: Minimization with a quadratic cost function

In this case, the objective function is the same in Case 2.1. The convergence of the total cost function is presented in Figure 9 (a). Table 6 shows an important improvement in total generation cost with three solar PV mega-structures with a quadratic cost function, ranging from 1454 $/h in Case 2.1 to 1307.8 $/h in this case. The total active power loss has lowered from 9.4010 MW in Case 2.1 to 5.1196 MW. The thermal generation cost is 850.218 $/h, which is considered 25.497 % lower than the obtained thermal generation cost in Case 2.1 and 52.414 % in Case 1.1. The bus voltage magnitudes are illustrated in Figure 10 where the minimum value is 0.9614 p.u at bus 38.

b. Case 3.2: Minimization with a cubic cost function

In this case, the objective function is the same in Case 2.2. The convergence of the total cost function is presented in Figure 9 (b). From Table 6, the simulation results of OPF with cubic cost function are better than those obtained with quadratic cost function. The total generation cost ranges from 1451 $/h in Case 2.2 to 1303.7 $/h. The thermal generation is 846.1317 $/h, which is considered 25.66 % lower than the thermal generation cost in Case 2.2 and 51.335 % in Case 1.2. Compared to Case 2.2, the total active power loss was reduced to 4.6563 MW from 9.2150 MW. The bus voltage magnitudes are illustrated in Figure 10 where the minimum value is 0.9020 p.u at bus 14.

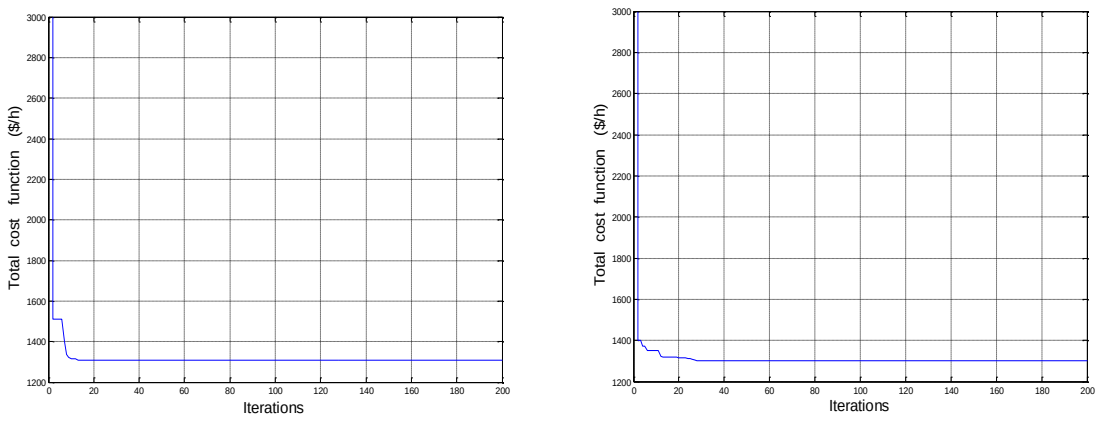

(a) (b)

Figure 9. Convergence of the total cost function with integration of three solar PV mega-structures.

Table 6. Simulation results with and without PV mega-structures.

Parameters	Case 1.1	Case 1.2	Case 2.1	Case 2.2	Case 3.1	Case 3.2
$P_{Th\ G\ 1}$	31.3292	31.5252	21.6707	25.2687	24.4897	23.2409
$P_{Th\ G\ 2}$	44.7764	49.9718	28.4512	28.3255	18.6727	23.5943
$P_{Th\ G\ 3}$	123.0342	109.4389	85.6654	80.6479	57.6990	47.2100
$P_{Th\ G\ 4}$	73.4139	122.2083	57.0025	58.4998	45.7435	49.2092
$P_{Th\ G\ 13}$	61.2325	27.5176	42.3868	42.9166	36.0299	35.0339
$P_{Th\ G\ 27}$	41.0186	23.8798	27.8938	29.3246	27.1968	14.3005
$P_{Th\ G\ 37}$	40.4049	58.6424	28.9401	25.1553	17.1827	27.9034
$P_{Th\ G\ 41}$	65.1655	42.0676	42.7632	46.4079	34.7007	19.2031
$P_{Th\ G\ 42}$	104.5974	136.2692	70.9612	70.7495	58.0934	68.3630
$P_{Th\ G\ 53}$	118.5920	101.0935	84.6487	82.9018	62.6131	73.8999
$P_{PV\ Tf}$	-	-	102.4969	102.4969	103.6784	103.6784
$P_{PV\ I}$	-	-	100.6205	100.6205	102.7326	102.7326
$P_{PV\ Tt}$	-	-	-	-	100.3872	100.3872
$V_{Th\ G\ 1}$	1.0881	1.0309	0.9504	0.9537	0.9905	0.9727
$V_{Th\ G\ 2}$	0.9725	1.0134	0.9502	1.0377	1.0707	0.9870
$V_{Th\ G\ 3}$	1.0879	1.0201	0.9694	1.0848	1.0255	0.9888
$V_{Th\ G\ 4}$	1.0848	1.0232	1.0429	0.9711	1.0058	1.0844
$V_{Th\ G\ 13}$	0.9633	0.9591	0.9503	1.0214	1.0854	0.9863
$V_{Th\ G\ 27}$	1.0867	1.0215	1.0600	1.0310	1.0763	0.9530
$V_{Th\ G\ 37}$	1.0725	1.0038	1.0028	0.9502	1.0797	1.0844
$V_{Th\ G\ 41}$	0.9656	0.9972	1.0417	1.0756	1.0303	0.9822
$V_{Th\ G\ 42}$	1.0870	1.0476	0.9726	0.9501	1.0432	1.0844
$V_{Th\ G\ 53}$	1.0876	1.0499	1.0421	0.9501	1.0302	0.9849
$V_{PV\ Tf}$	-	-	0.9984	1.0837	0.9523	0.9628
$V_{PV\ I}$	-	-	1.0771	0.9914	1.0285	0.9736
$V_{PV\ Tt}$	-	-	-	-	0.9969	0.9843
P_{Loss} (MW)	19.4648	18.5143	9.4010	9.2150	5.1196	4.6563
C_{Th} ($/h)	1786.7	1738.7	1141.2	1138.2	850.2180	846.1317
C_{PV} ($/h)	-	-	312.8543	312.8543	457.6099	457.6099
C_{tot} ($/ h)	-	-	1454.00	1451.00	1307.80	1303.70

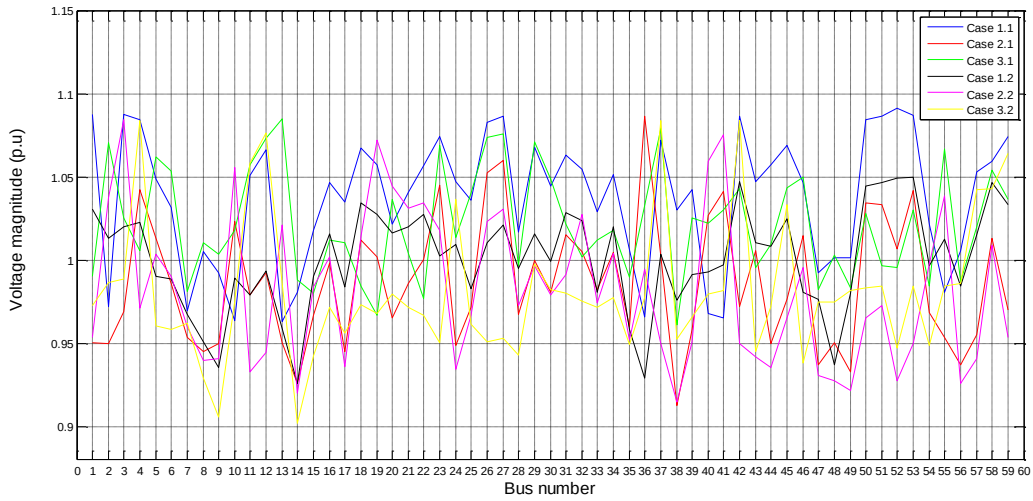

Figure 10. Voltage profile of the test system with and without integration of solar PV mega-structures.

6.4. Simultaneous minimization of generation cost and emissions without solar PV mega-structures

In this case, the OPF is solved for simultaneous reducing of generation cost and emissions by considering only 10 thermal generators. The objective function to be minimized is given by Equation (13) with $w_f = 0.5$. The results are presented in Table 7.

a. Case 4.1: Minimization with a quadratic cost function

The goal in this case is to reduce the thermal generation cost and emissions with a quadratic cost function. The convergence of the emission function is shown in Figure 11(a). From Table 7, the thermal generation cost and emission are 1784.5 $/h and 0.4348 Ton/h, respectively. The total active power loss is 19.5798 MW. The bus voltage magnitudes are illustrated in Figure 13, where the minimum value is 0.9097 p.u at bus 14.

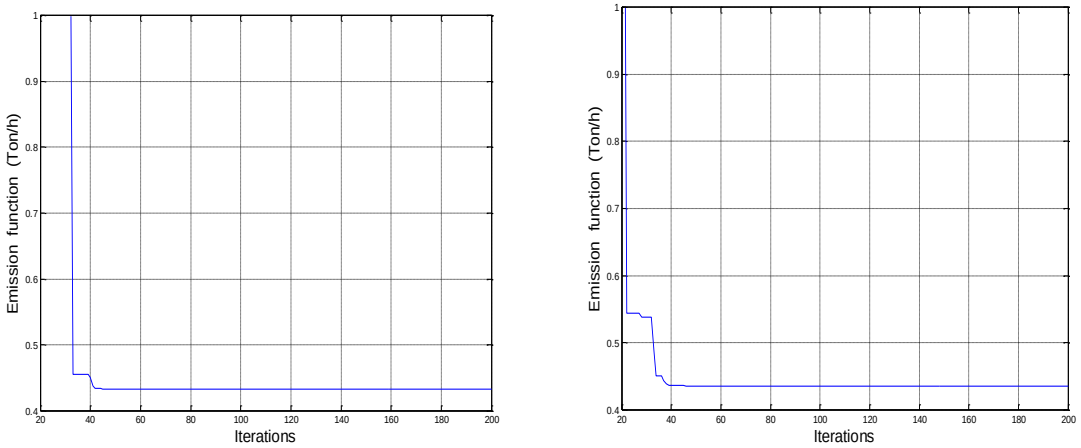

(a) (b)

Figure 11. Convergence of the emission function without integration of solar PV mega-structures.

b. Case 4.2: Minimization with a cubic cost function

The main objective in this case is to reduce simultaneously the thermal generation cost and emissions with a cubic cost function. The convergence of the emission function is shown in Figure 11 (b). From Table 7, the simulation results of OPF with cubic cost function are better than those obtained with quadratic cost function. The obtained thermal generation cost and emission are 1782.7 $/h and 0.4325 Ton/h, respectively. The total active power loss is 18.9257 MW. The bus voltage magnitudes are illustrated in Figure 13, where the minimum value is 0.9074 p.u at bus 14.

6.5. Simultaneous minimization of generation cost and emissions with integration of solar PV mega-structures

In this case, the OPF is solved to minimize simultaneously the total generation cost and emissions with the integration of two PV mega-structures. The objective function is given by Equation (14) with $w_f = 0.5$. The two mega-structures are connected to 59 bus test system at buses 19 and 36 in Tindouf and Illizi cities, respectively. Table 7 presents the results.

a. Case 5.1: Minimization with a quadratic cost function

The objective in this case is to reduce the total generation cost and emissions with a quadratic cost function. The convergence of the emission function is shown in Figure 12 (a). From Table 7, it can be observed that there is an improvement in emission, generation cost, and total active power loss, with the integration of solar PV mega-structures. The obtained thermal generation cost and emission are 1117 $/h and 0.3950 Ton/h, respectively. The thermal generation cost is considered 37.405 % lower than the cost in Case 4.1. The emission is considered 9.1536 % lower than the emission in Case 4.1. The total active power loss has reduced from 19.5798 MW in Case 4.1 to 9.4556 MW. The bus voltage magnitudes are illustrated in Figure 13, where the minimum value is 0.9255 p.u at bus 14.

b. Case 5.2: Minimization with a cubic cost function

The goal in this case is to minimize the total generation cost and emissions with a cubic cost function. Figure 12 (b) illustrates the convergence of the emission function. Table 7 demonstrates that OPF results using a cubic cost function are better than those using a quadratic cost function. The obtained thermal generation cost and emission are 1115.5 $/h and 0.3944 Ton/h, respectively. The obtained thermal generation cost is considered 37.426 % lower than the cost in Case 4.2. The obtained emission is considered 8.809 % lower than the emission in Case 4.2. The total active power loss has lowered from 18.9257 MW in Case 4.2 to 9.3610 MW. The bus voltage magnitudes are illustrated in Figure 13, where the minimum value is 0.9371 p.u at bus 11.

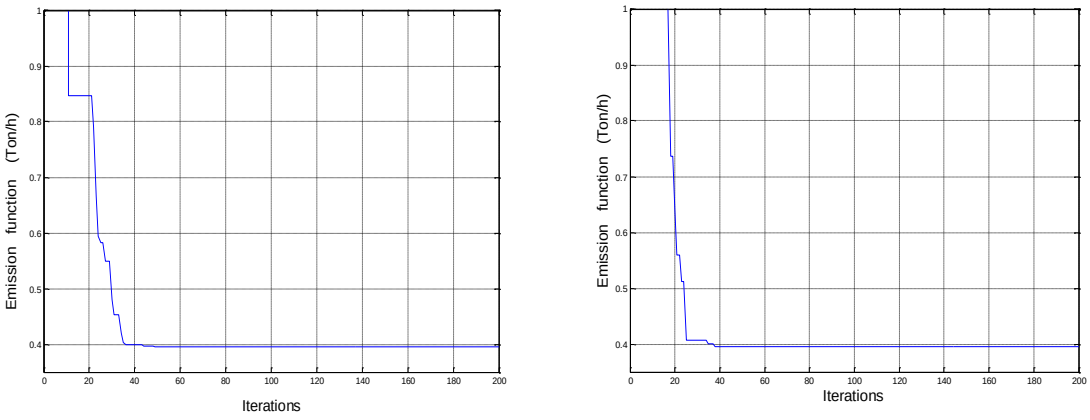

(a) (b)

Figure 12. Convergence of the emission function with integration of two solar PV mega-structures.

Table 7. Simulation results with and without considering PV mega-structures.

Parameters	Case 4.1	Case 4.2	Case 5.1	Case 5.2
$P_{Th\ G\ 1}$	32.8959	31.7843	23.2187	23.7896
$P_{Th\ G\ 2}$	39.8419	38.9566	28.9032	27.9133
$P_{Th\ G\ 3}$	125.7193	123.1953	87.6102	86.5698
$P_{Th\ G\ 4}$	80.1877	81.5281	57.8967	57.7327
$P_{Th\ G\ 13}$	59.7503	59.2818	43.7165	43.0160
$P_{Th\ G\ 27}$	38.5248	40.4916	28.5738	29.1108
$P_{Th\ G\ 37}$	41.7966	41.6771	27.9182	27.5275
$P_{Th\ G\ 41}$	60.0736	60.8745	42.2146	43.6317
$P_{Th\ G\ 42}$	99.7923	103.5497	50.7870	51.6037
$P_{Th\ G\ 53}$	125.0974	121.6866	86.9713	86.8205
$P_{PV\ Tf}$	-	-	106.3015	106.3015
$P_{PV\ I}$	-	-	109.4439	109.4439
$V_{Th\ G\ 1}$	1.0014	1.0386	0.9852	1.0523
$V_{Th\ G\ 2}$	0.9901	0.9702	1.0857	1.0199
$V_{Th\ G\ 3}$	1.0551	1.0498	1.0016	0.9993
$V_{Th\ G\ 4}$	1.0149	0.9646	0.9897	1.0712
$V_{Th\ G\ 13}$	0.9853	1.0500	0.9832	1.1000
$V_{Th\ G\ 27}$	1.0038	0.9579	1.0204	1.0664
$V_{Th\ G\ 37}$	0.9896	1.0024	1.0028	0.9512
$V_{Th\ G\ 41}$	1.0139	0.9991	1.0122	0.9983
$V_{Th\ G\ 42}$	1.0076	1.0368	1.0374	1.0148
$V_{Th\ G\ 53}$	1.0364	0.9983	1.0031	1.0077
$V_{PV\ Tf}$	-	-	1.0992	1.0834
$V_{PV\ I}$	-	-	1.0216	0.9510
P_{Loss} (MW)	19.5798	18.9257	9.4556	9.3610
C_{Th} ($/h)	1784.50	1782.70	1117.00	1115.50
C_{PV} ($/h)	-	-	243.4003	243.4003
E (Ton/h)	0.4348	0.4325	0.3950	0.3944

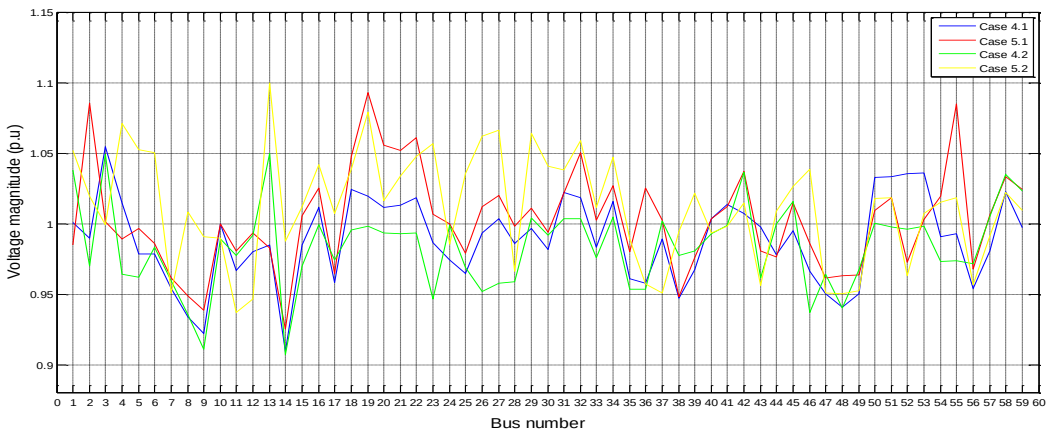

Figure 13. Voltage profile of the test power system with and without integration of solar PV mega-structures

7. CONCLUSION

This article shows that southern Algeria is among the sunniest regions on Earth with very interesting solar potential for internal and beyond national borders use.

According to this vision, a reorientation of the power flows of the Algerian electrical transmission network integrating mega photovoltaic structures was proposed. Even if their necessary location in the south presents technical constraints due to the desert relief conditions, it remains crucial to satisfy the new strategic objectives, especially the oligopolistic one that ensures the sustainability of energy needs, since forecasts confirm the continued decline of fossil sources. For this, it was admitted that the suitable research methodology in these conditions would be the OPF based PSO algorithm. The OPF model considers quadratic and cubic thermal cost functions and the uncertainties of solar energy are modeled by βPDF.

An Algerian 59 bus test system with some advantageous choices of solar power source locations, has been considered. Five cases have been evaluated, and the results of the simulation indicate that the active powers of generators and the bus voltage magnitudes remain within permissible limits. The case of the cubic thermal cost function allows a significant reduction of environmental pollution while satisfying the power demand growth of interconnected power networks.

Thanks to the properties of the PSO algorithm used for OPF resolution, it could be stated that the Algerian solar field seems to be a good opportunity for large-scale PV installations in an oligopolistic and environmentally friendly sense.

ACKNOWLEDGMENTS

We appreciate the support of the electrical laboratory of Skikda (Laboratoire d'Electrotechnique de Skikda 'LES').

REFERENCES

[1] H. J. Touma, M. Mansor, M. S. Abd Rahman, H. Mokhlis and Y. J. Ying, "Influence of Renewable Energy Sources on Day Ahead Optimal Power Flow Based on Meteorological Data Forecast Using Machine Learning : A Case Study of Johor Province", *Indonesian Journal of Electrical Engineering and Informatics (IJEEI),* Vol. 11, No. 1, pp. 225~240, March 2023.

[2] F.M. Tuaimah and M.F. Meteb, "A Linear Programming Method Based Optimal Power Flow Problem for Iraqi Extra High Voltage Grid (EHV)", *Journal of Engineering*, Vol. 20, 2014.

[3] O.D. Montoya, W. Gil-González and J.C. Hernández, "Optimal Power Flow Solution for Bipolar DC Networks Using a Recursive Quadratic Approximation", *Energies*, Vol. 16, 2023.

[4] C. M. Wankhade and A. P. Vaidya, "Optimal Power Flow Using Genetic Algorithm: Parametric Studies for Selection of Control and State Variables", *British Journal of Applied Science & Technology*, pp. 279-301, 2014.

[5] T. Kulworawanichpong, "Optimal power flow solution using adaptive tabu search", *International Journal of the Physical Sciences,* Vol. 6, pp. 6394-6409, 2011.

[6] C. Shilaja and K. Ravi, "Optimal Power Flow Considering Intermittent Wind Power Using Particle Swarm Optimization", *International Journal of Renewable Energy Research,* Vol.6, No. 2, 2016.

[7] M.A. Abido, "Optimal power flow using particle swarm optimization", *Electrical Power Energy System*, Vol. 24, pp. 563-571, 2002.

[8] K. Cherukupalli, P. Raju Chinda and S. Peddakotla, "Security Constrained Optimal Power Flow by Hybrid SATS Algorithm", *Research in Dynamical & Control Systems*, Vol. 10, 2018.

[9] X. He, W. Wang, J. Jiang and L. Xu, "An Improved Artificial Bee Colony Algorithm and Its Application to Multi-Objective Optimal Power Flow", *Energies,* Vol. 8, pp: 2412–2437, 2015.

[10] K. Lenin, B. R. Reddy, and M. Surya Kalavathi, "Optimal Power Flow using Ant Colony Search Algorithm to Evaluate Load Curtailment Incorporating Voltage Stability Margin Criterion", *International Journal of Electrical and Computer Engineering (IJECE),* Vol. 3, pp. 603-611, 2013.

[11] A. Harrouz, A. Temmam and M. Abbes, "Renewable Energy in Algeria and Energy Management Systems", *International Journal of Smart Grid*, Vol. 2, No. 1, 2018.

[12] S. Pahlavan, M. Jahangiri, A. Shamsabadi, and A. Khechekhouche "Feasibility study of solar water heaters in Algeria, a review", *Journal of Solar Energy Research*, Vol 3, No. 2, pp: 135-146, 2018.

[13] U.S. Energy Information Administration, "Country Analysis Brief: Algeria", March 2023.

[14] Brahim Bergougui, "Moving toward environmental mitigation in Algeria: Asymmetric impact of fossil fuel energy, renewable energy and technological innovation on CO2 emissions", *Energy Strategy Reviews*, Vol. 51, January 2024.

[15] ALGERIE Eco, "Consommation d'électricité : nouveau pic historique de plus de 18.476 mégawatts", Juillet 2023.

[16] Nova News, "Algeria wants to export eight gigawatts of electricity to Europe", December 2022.

[17] International Renewable Energy Agency IRENA, "Energy profil, Algeria", August 2023.

[18] Ministère de l'Energie, CREG, "Les énergies renouvelables en Algérie", *Ministère de l'Energie, CREG*, Berlin, 2016.

[19] Reuters, "Algeria suggests to sell spare electricity capacity to Europe -president", December 2022.

[20] Algérie presse service, "Sonelgaz : lancement du projet d'interconnexion du réseau électrique du sud avec le réseau national", Mai 2023.
[21] A. Chabani, S. Makhloufi, S. Lachtar, "Overview and impact of the renewable energy plants connected to the electrical network in southwest Algeria", *EAI Endorsed Transactions on Energy Web*, Vol. 8, Issue 36, 2021.
[22] B. Bousshoua and A. Elmaouhab, "Smart Grid Reliability Using Reliable Block Diagram Case Study: Adrar's Isolated", *International Conference on Power Generation Systems and Renewable Energy Technologies (PGSRET)*, August 2019.
[23] M.R. Yaiche and A. Bouhanik, "Atlas solaire Algérien", 2002.
[24] M. R. Yaiche, A. Bouhanik, S. M. A. Bekkouche, and T. Benouaz, "A new modelling approach intended to develop maps of annual solar irradiation and comparative study using satellite data of Algeria", *Journal of Renewable and Sustainable Energy* 8, 2016.
[25] G.A. Ajenikoko, Olakunle and E. Olabode, " Optimal Power Flow with Reactive Power Compensation for Cost And Loss Minimization On Nigerian Power Grid System", *Indonesian Journal of Electrical Engineering and Informatics (IJEEI)*, Vol. 5, No. 3, pp. 236~247, September 2017.
[26] P. Biswas, P.N. Suganthan and G. Amaratunga, "Optimal power flow solutions incorporating stochastic wind and solar power", *Energy Conversion and Management*, pp.1194-1207, 2017.
[27] S. Surender Reddy, "Multi-Objective Optimal Power Flow for a Thermal-Wind-Solar Power System", *Journal of Green Engineering*, Vol. 7, pp. 451–476**,** 2018.
[28] A.S. Alghamdi, "Optimal Power Flow of Renewable-Integrated Power Systems Using a Gaussian Bare-Bones Levy-Flight Firefly Algorithm" *Frontiers in Energy Research*, Vol. 10, 2022.
[29] A. Mallem and O. Boudebbouz, "Economic Dispatch on a Power System Network Interconnected with Solar Farm*", In the IEEE proceedings, 1st International Conference on Sustainable Renewable Energy Systems and Applications*, Tebessa, Algeria, 2019.
[30] J. Kennedy and R. Eberhart, "Particle swarm optimization", *Proc. IEEE Int. Conf. on Neural Networks*, Vol. 4, pp: 1942–1948, Australia, 1995.
[31] R. Eberhart and J. Kennedy, "A new optimizer using particle swarm theory", *Proc. IEEE 6th Int. Conf. Symposium on Micro Machine and Human Science*, pp. 39-43, Japan, 1995.
[32] B. Bentouati, L. Chaib and S. Chettih, "Optimal Power Flow using the Moth Flam Optimizer: A Case Study of the Algerian Power System", *Indonesian Journal of Electrical Engineering and Computer Science*, Vol. 1, No.3, pp: 431- 445, 2016.
[33] B. Mahdad, T. Bouktir and K. Srairi, "OPF with Envirenmental Constraints with SVC Controller using Decomposed Parallel GA: Application to the Algerian Network", *Journal of Electrical Engineering and technology*, Vol. 4, No. 1, pp. 55-65, 2009.